Articles

Auto-organization of Nanostructured Organic−Inorganic Hybrid Xerogels Prepared by Sol−Gel Processing: The Case of a "Twisted" Allenic Precursor

Geneviève Cerveau, Robert J. P. Corriu,* Eric Framery, and Frédéric Lerouge

Laboratoire de Chimie Moléculaire et Organisation du solide, UMR 5637, Université Montpellier II, cc 007, Place E. Bataillon, F-34095 Montpellier Cedex 5, France

Received June 11, 2004. Revised Manuscript Received July 22, 2004

Nanostructured hybrid materials prepared by sol−gel hydrolysis−polycondensation of the precursor 1,3-bis(propyltrimethoxysilyl)-1,3-diphenylallene **P** having a bulky rigid and twisted core with two short flexible arms exhibited a self-organization evaluated by birefringence measurements (micrometric scale) and X-ray diffraction studies (nanometric scale). These observations show that the auto-organization of hybrid materials is not limited to rigid-rod or mesogenic spacers. It appears as a more general phenomenon. The twisted geometry of the organic group induced an anisotropic organization, the morphology of which was unprecedented and different from the one observed with the linear or mesogenic hybrid materials previously studied. Moreover, the birefringence pictures were also different from those observed with liquid crystals. In some cases unprecedented wavy parallel cracks showed the extension of the organization over the millimetric scale. It is the same for the X-ray diffraction. In all the cases precedently studied the X-ray diffraction diagrams exhibit diffraction peaks related to the length of the organic spacer. We observed here signals which did not correspond to this distance, suggesting a different nanometric scale organization in the solid.

Introduction

The hydrolytic sol−gel polycondensation is a very convenient method to prepare silica-based organic−inorganic materials.[1−5] The choice of the organic unit is very broad, permitting the formation of materials with physical and chemical properties: NLO materials,[6,7] luminescent materials,[8−11] and also mesoporous and PMOS materials.[12−18] Contrary to silica, which is always amorphous when prepared by the sol−gel method, the possibility of self-organization in these hybrid materials has been demonstrated by using very specific organic precursors such as octadecyltrichlorosilane,[19] chiral diureidocyclohexane,[20] or a bisurea-based[21] precursor that exhibit a strong interaction by H-bonding. A long-range organization has also been achieved by a solid-state approach.[22−24] Even when all the silica materials obtained by the sol−gel route are always amorphous systems, we have previously observed that the organic−inorganic hybrid materials prepared according to Scheme 1 present an organization at the nanometric scale as evidenced by X-ray powder diffraction as well as an

* To whom correspondence should be addressed. E-mail: corriu@univ-montp2.fr.

(1) Brinker, C. J.; Scherer, G. W. *Sol−Gel Science: The Physics and Chemistry of Sol−Gel Processing*; Academic Press: San Diego, 1990.
(2) Loy, D. A.; Shea, K. J. *Chem. Rev.* **1995**, *95*, 1431.
(3) Corriu, R. J. P. *Angew. Chem., Int. Ed.* **2000**, *39*, 1376.
(4) de Soler-Illia, G. J.; Sanchez, C.; Lebeau, B.; Patarin, J. *Chem. Rev.* **2002**, *102*, 4093.
(5) Sanchez, C.; de Soler-Illia, G. J.; Ribot, F.; Grosso, D. *C. R. Chim.* **2003**, *6*, 1131.
(6) Toussaere, E.; Zyss, J.; Griesmar, P.; Sanchez, C. *Nonlinear Opt.* **1991**, *1*, 349.
(7) Yang, Z.; Xu, C.; Wu, B.; Dalton, L. R.; Kalluri, S.; Steier, W. H.; Shi, Y.; Bechtel, J. H. *Chem. Mater.* **1994**, *6*, 1899.
(8) Shea, K. J.; Loy, D. A.; Webster, O. *J. Am. Chem. Soc.* **1992**, *114*, 6700.
(9) Corriu, R. J. P.; Hesemann, P.; Lanneau, G. F. *Chem. Commun.* **1996**, 1845.
(10) Franville, A. C.; Zambon, D.; Mahiou, R.; Chou, S.; Troin, Y.; Cousseins, J. C. *J. Alloys Compd.* **1998**, *275−277*, 831.
(11) Franville, A.-C.; Zambon, D.; Mahiou, R.; Troin, Y. *Chem. Mater.* **2000**, *12*, 428.
(12) Melde, B. J.; Holland, B. T.; Blanford, C. F.; Stein, A. *Chem. Mater.* **1999**, *11*, 3302.
(13) Stein, A.; Melde, B. J.; Schroden, R. C. *Adv. Mater.* **2000**, *12*, 1403.
(14) Ying, J. Y.; Mehnert, C. P.; Wong, M. S. *Angew. Chem., Int. Ed.* **1999**, *38*, 56.
(15) MacLachlan, M. J.; Asefa, T.; Ozin, G. A. *Chem. Eur. J.* **2000**, *6*, 2507.
(16) Asefa, T.; Yoshina-Ishii, C.; MacLachlan, M. J.; Ozin, G. A. *J. Mater. Chem.* **2000**, *10*, 1751.
(17) Inagaki, S.; Guan, S.; Fukushima, Y.; Ohsuna, T.; Terasaki, O. *J. Am. Chem. Soc.* **1999**, *121*, 9611.
(18) Inagaki, S.; Guan, S.; Ohsuna, T.; Terasaki, O. *Nature* **2002**, *416*, 304.
(19) Shimojima, A.; Sugahara, Y.; Kuroda, K. *J. Am. Chem. Soc.* **1998**, *120*, 4528.
(20) Moreau, J. J. E.; Vellutini, L.; Man, M. W. C.; Bied, C. *J. Am. Chem. Soc.* **2001**, *123*, 1509.
(21) Moreau, J. J. E.; Vellutini, L.; Man, M. W. C.; Bied, C.; Bantignies, J.-L.; Dieudonné, P.; Sauvajol, J.-L. *J. Am. Chem. Soc.* **2001**, *123*, 7957.
(22) Boury, B.; Ben, F.; Corriu, R. J. P. *Angew. Chem., Int. Ed.* **2001**, *40*, 2853.
(23) Cerveau, G.; Chappellet, S.; Corriu, R. J. P. *J. Mater. Chem.* **2003**, *13*, 1905.
(24) Cerveau G, Chappellet, S., Corriu R. J. P, Dabiens B. *Silicon Chem.* **2002**, *1*, 321.

10.1021/cm049061c CCC: $27.50
Published on Web 09/04/2004

Scheme 1

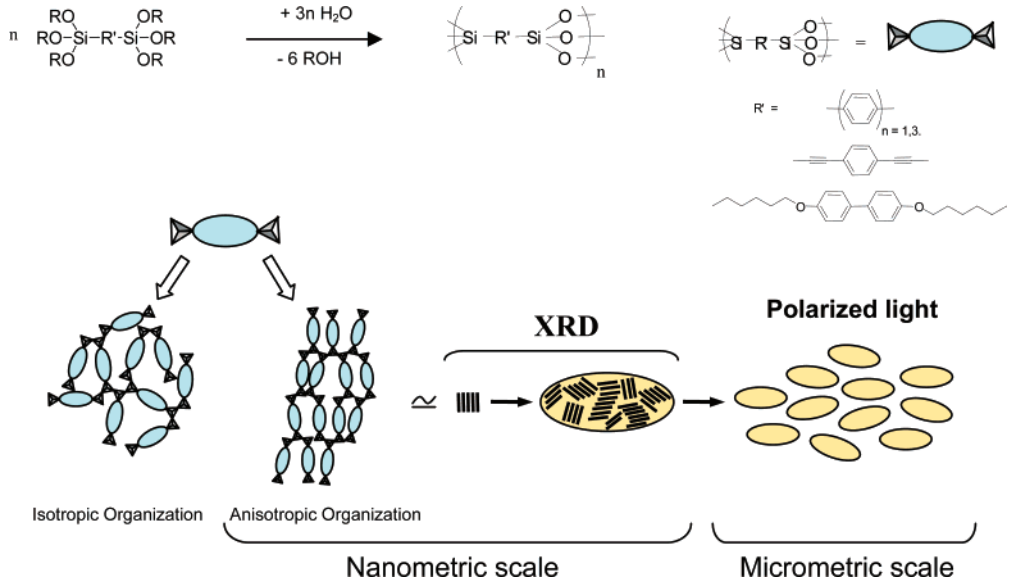

organization at the micrometric scale shown by birefringence experiments.[25] Thus, the introduction of an organic group appeared like a factor favorable for the existence of an organization into these amorphous systems since the X-ray scattering exhibits diffraction signals, but never any Bragg peak. Until now, all the systems that have been studied correspond to linear spacers presenting rigid or semirigid or flexible geometries.[25−27] In all the cases investigated, only weak interactions between the organic moieties such as van der Waals, London, or $\pi-\pi$ stacking were able to induce an organization. All the solids presented an organization at the nanometric scale (X-ray diffraction) and at the micrometric one (birefringence) with the exception of the flexible aliphatic spacers $(CH_2)_n$.[28] Studies of the organization as a function of the experimental conditions clearly show a kinetic control as evidenced by modifications of X-ray diagrams and birefringence pictures (intensity and geometry) depending on parameters such as concentration of precursor, concentration of catalyst, solvent, and catalyst.[25] Thus, the structure as well as the texture of the hybrid solids are under kinetic control.[29] Moreover, the X-ray study as a function of the size of the rigid spacer clearly shows a correlation between the length of the organic group and the diffraction patterns. This is also observed in the case of semirigid spacers.[26,27,30] Thus, this set of observations was worth studying the limits of this phenomenon. What type of geometry allows an organization? We describe here the study of a twisted linear precursor exhibiting an order 2 axis, the 1,3-bis(propyltrimethoxysilyl)-1,3-diphenylallene **P**. This compound has a bulky rigid and twisted core with two short flexible arms (Scheme 2). In contrast to the mesogenic precursors

Scheme 2

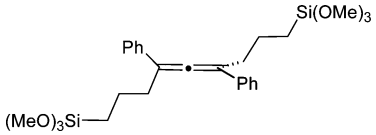

(rigid nontwisted aromatic structure and long flexible arms), with such a geometry we were expecting either a poor organization or something very different from the previous precursors.[31] We have focused on the effect of the experimental conditions for the preparation of the xerogels on their structure, texture, and organization. We have studied the influence of concentrations of both the precursor and the catalyst and also the effect of temperature.

Experimental Section

All reactions were carried out under argon using a vacuum line and Schlenk techniques. Solvents were dried and distilled just before use. The ^{1}H and ^{13}C NMR spectra were recorded on a Bruker DPX-200 spectrometer and the ^{29}Si NMR spectra were recorded on a Bruker WP-200 SY spectrometer. The ^{29}Si CP MAS NMR spectra were recorded on a Bruker Advance DPX 400. Chemical shifts are given relative to tetramethylsilane. The mass spectra were obtained with a high-resolution mass spectrometer Varian MAT 311. The X-ray experiments were performed, in the Physics Department, on powders of solids in a Lindeman tube with an imaging plate 2D detector with a rotating anode apparatus. The radiation used was Cu Kα (λ = 1.5418 Å). Optical properties of the materials were observed with a Laborlux12POLS polarizing microscope. Photographs were taken using a Leica wild MPS28 camera. The birefringence Δn of the gels was obtained from the expression $\Delta l = (\Delta n)d$, where Δl is the optical path difference and d is the cell thickness which is evaluated by UV−vis spectroscopy (15 ± 2 μm). Δl was measured by a Berek compensator. Elemental analyses were carried out by the "Service Central de Micro-Analyse du CNRS". (*tert*-Butyldimethyl[(1-phenylmethyl-2-phenylethenyl)oxy]silane) (**1**) was prepared according to literature procedure.[32]

(25) Boury, B.; Ben, F.; Corriu, R. J. P.; Delord, P.; Nobili, M. *Chem. Mater.* **2002**, *14*, 730.
(26) Boury, B.; Corriu, R. *Chem. Rec.* **2003**, *3*, 120 and references cited therein.
(27) Boury, B.; Corriu, R. J. P. *Chem. Commun.* **2002**, 795 and references cited therein.
(28) Ben, F.; Boury, B.; Corriu, R. J. P.; Le Strat, V. *Chem. Mater.* **2000**, *12*, 3249.
(29) Cerveau, G.; Corriu, R. J. P.; Framery, E. *Chem. Mater.* **2001**, *13*, 3373.
(30) Boury, B.; Corriu, R. J. P. In *Supplement Si: The Chemistry of Organic Silicon Compounds;* Rappoport, Z., Apeloig, Y., Eds.; Wiley & Sons: Chichester, 2001; Chapter 10, p 565.
(31) Ben, F.; Boury, B.; Corriu, R. J. P. *Adv. Mater.* **2002**, *14*, 1081.

Scheme 3

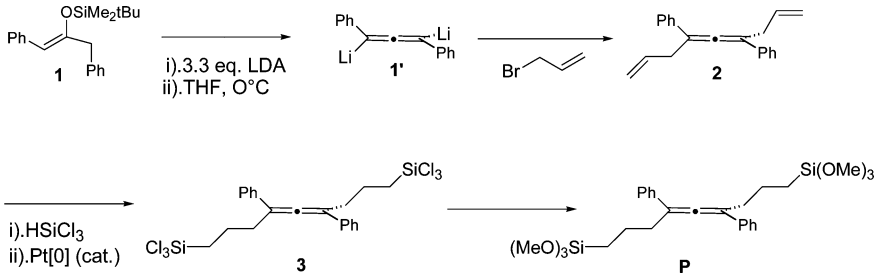

1,3-Bis(allyl)-1,3-diphenylallene (2). To a solution of LDA (19.8 mmol, 3.3 molar equivalent) in THF (50 mL) [prepared by addition of *n*BuLi (14.5 mL) to a solution of diisopropylamine (3 mL) in THF] was added a solution of **1** (1.95 g, 6 mmol) in THF (10 mL) at 0 °C. The ice bath was removed and the color of the solution turned deep red. After stirring for 6 h at room temperature, a solution of allyl bromide (2.54 g, 21 mmol, 3.5 equiv) in THF (10 mL) was added at 0 °C. The orange solution was stirred for 12 h at 20 °C. The solvent was removed in a vacuum to obtain a solid, which was extracted with hexane (3 × 50 mL). Precipitation of LiBr was observed. The extracts were filtered through Celite and the solvent was removed in a vacuum. The crude product was purified by column chromatography (Alumine, hexane) to give **2** as a light yellow oil (1.34 g, 4.92 mmol, 82%). Elemental analysis calcd (%) for $C_{21}H_{20}$: C, 92.60; H, 7.40. Found: C, 91.90; H, 7.35. ^{1}H NMR (200 MHz, $CDCl_3$) δ (ppm): 3.51 (m, 4 H; CH_2); 5.19 (m, 2 H; CH═); 6.05 (m, 4 H; ═CH_2); 7.65 (m, 5H, C_6H_5); 7.73 (m, 5H, C_6H_5). ^{13}C NMR (50 MHz, $CDCl_3$) δ (ppm): 35.55 (**C**H_2-$CHCH_2$); 115.32 (**C**H═CH_2); 121.12 (CH═**C**H_2); 123.28 (═**C**-CH_2); 125.56 (Ar); 127.41 (Ar); 130.08 (Ar); 132.87 (Ar); 207.45 (═C═). Electronic impact: *m*/*z* 271.1453, [M+.]. Calcd for $(C_{21}H_{19})^+$: 271.1486.

1,3-Bis(propyltrimethoxysilyl)-1,3-diphenylallene (P). This hydrosilylation of **2** was a neat reaction. To a solution of allene **2** (1.76 g, 6.45 mmol) dissolved in trichlorosilane (4.37 g, 32.25 mmol, 5 molar equivalent) was added a few drops of Karstedt's catalyst. The brownish solution was stirred a few hours at room temperature. Excess of trichlorosilane was removed under vacuum to give **3** as a crude product which was converted into **P** without further purification. **3**: (3.21 g, 5.8 mmol, 90%). ^{1}H NMR (200 MHz, $CDCl_3$) δ (ppm): 0.72 (m, 4 H; CH_2), 1.16 (m, 4 H; CH_2), 1.93 (m, 4 H; CH_2), 7.38 (m, 5H, C_6H_5), 7.47 (m, 5H, C_6H_5).

MeOH (1.67 g, 52 mmol, 9 molar equivalent) was added to a solution of **3** (3.21 g, 5.8 mmol) in hexane (50 mL). A solution of Et_3N (5.26 g, 52 mmol, 9 molar equivalent) in hexane (50 mL) was added and white fumes with precipitate were observed. After the solution was stirred for 5 h at room temperature, the milky mixture was filtered. Hexane was removed under vacuum to give **P** as a yellow oil (2.48 g, 4.8 mmol, 83%). Elemental analysis: calcd (%) for $C_{27}H_{40}O_6Si_2$: C, 62.75; H, 7.80; Si, 10.87. Found: C, 62.08; H, 7.85; Si, 10.62. ^{1}H NMR (200 MHz, $CDCl_3$) δ (ppm): 0.65 (m, 4 H; CH_2), 1.25 (m, 4 H; CH_2), 1.93 (m, 4 H; CH_2), 3.53 (s, 18H; CH_3O), 7.35 (m, 5H, C_6H_5), 7.53 (m, 5H, C_6H_5). ^{13}C NMR (50 MHz, $CDCl_3$) δ (ppm): 9.45 (Si**C**H_2), 18.76 (CH_2**C**H_2CH_2), 46.64 (**C**H_2CH═), 50.70 (OCH_3); 124.38 (Ar), 124.65 (Ar), 128.52 (Ar), 131.97 (Ar), 143.93 (C═), 207.45 (═C═). ^{29}Si NMR (39 MHz, $CDCl_3$) δ (ppm): −41.55. Electronic impact: *m*/*z* 516.2366 [M+.]. Calcd for $(C_{27}H_{40}O_6Si_2)^+$: 516.2363.

Preparation of the Xerogels X. The preparation of the xerogels was carried out according to the following general procedure. The yields (based on a totally polycondensed solid) were almost quantitative in all cases. Some of them were over 100% due to the presence of remaining Si−OR groups (R═H or Me). The preparation of the xerogel **X1** is given as an example: In a Schlenk tube 0.8 g (1.55 mmol) of **P** and 774 μL of dried THF were introduced. 774 μL of a solution containing 31 μL (31 μmol) of TBAF (1 mol L^{-1} in THF), 84 μL (4.64 mmol) of H_2O, and 659 μL of dried THF were added. After homogenization, a part of this mixture was introduced by capillarity into the cell, and the remaining solution was kept in the Schlenk tube. In the two cases, after the sol−gel transition, the translucent gel was aged 6 days. Then, the gel obtained in the Schlenk tube was crashed and washed twice with acetone, ethanol, and diethyl ether, and the resulting solid was dried at 120 °C in vacuo for 3 h, yielding a white powder.

X1: 0.615 g (1.53 mmol). Yield = 98%. ^{29}Si CP MAS NMR (δ ppm, 60 MHz): −56.2 (T^2); −65.7 (T^3). S_{BET} < 10 m^2 g^{-1}.

X2: 0.8 g (1.55 mmol) of **P** in 1.55 mL of THF containing 8 μL of TBAF and 34 μL of H_2O gave a gel after 20 min. **X2**: 0.608 g (1.51 mmol). Yield = 97%. ^{29}Si CP MAS NMR (δ ppm, 60 MHz): −48.5 (T^1); −58.4 (T^2); −64.8 (T^3). S_{BET} < 10 m^2 g^{-1}.

X3: 0.5 g (0.97 mmol) of **P** in 968 μL of THF containing 2 μL of TBAF and 52 μL of H_2O gave a gel after 90 min. **X3**: 0.370 g (0.92 mmol). Yield = 95%. ^{29}Si CP MAS NMR (δ ppm, 60 MHz): −48.3 (T^1); −57.4 (T^2); −65.6 (T^3). S_{BET} < 10 m^2 g^{-1}.

X4: 0.7 g (1.42 mmol) of **P** in 474 μL of THF containing 7 μL of TBAF and 78 μL of H_2O gave a gel after 7−8 min. **X4**: 0.584 g (1.45 mmol). Yield = 102%. ^{29}Si CP MAS NMR (δ ppm, 60 MHz): −48.4 (T^1); −57.3 (T^2); −64.8 (T^3). S_{BET} < 10 m^2 g^{-1}.

X5: 0.5 g (0.97 mmol) of **P** in 322 μL of THF containing 2 μL of TBAF and 52 μL of H_2O gave a gel after 45 min. **X5**: 0.410 g (1.02 mmol). Yield = 105%. ^{29}Si CP MAS NMR (δ ppm, 60 MHz): −47.6 (T^1); −56.5 (T^2); −65.2 (T^3). S_{BET} < 10 m^2 g^{-1}.

X6: 0.5 g (0.97 mmol) of **P** in 968 μL of THF containing 2 μL of TBAF and 52 μL of H_2O, at 3 °C, gave a gel after 14 days. **X6**: 0.362 g (0.90 mmol). Yield = 93%. ^{29}Si CP MAS NMR (δ ppm, 60 MHz): −41.92 (T^0); −47.9 (T^1); −56.6 (T^2); −65.1 (T^3). S_{BET} < 10 m^2 g^{-1}.

Results and Discussion

Synthesis of Precursor P. Among the number of methods for the synthesis of allenes, a new one was recently reported.[32] It consists of the direct transformation of silyl enol ethers into functionalized allenes. Compound **P** was prepared by this route in three steps starting from *tert*-butyldimethyl[(1-phenylmethyl-2-phenylethenyl)oxy]silane (**1**)[32] (Scheme 3). In a first step addition of a solution of **1** in THF to a solution of 3.3 equiv of lithium diisopropylamide (LDA) in THF led to the formation of a 1,3-dilithioallene intermediate **1′**, which was then directly treated by allylbromide to give 1,3-bis(allyl)-1,3-diphenylallene (**2**) in 82% yield. The second step was the hydrosilylation reaction[33] of **2** with $HSiCl_3$ in the presence of Karstedt's catalyst,[34,35] which led to 1,3-bis(propyltrichlorosilyl)-1,3-diphenylallene **3**

(32) Langer, P.; Doring, M.; Seyferth, D.; Gorls, H. *Chem. Eur. J.* **2001**, *7*, 573.

(33) Ojima, I. *Chem. Org. Silicon Compd.* **1989**, *2*, 1479.

(34) Hitchcock, P. B.; Lappert, M. F.; Warhurst, N. J. W. *Angew. Chem.* **1991**, *103*, 439.

(35) Faglioni, F.; Blanco, M.; Goddard, W. A., III.; Saunders, D. *J. Phys. Chem. B* **2002**, *106*, 1714.

Scheme 4

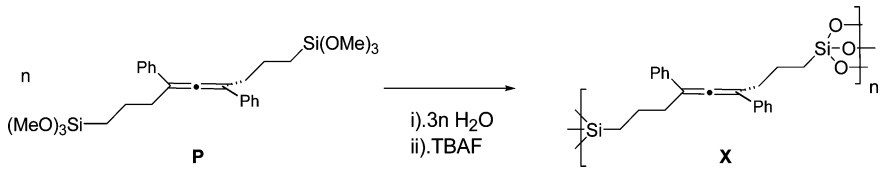

Table 1. Experimental Conditions, ^{29}Si CP MAS NMR Data, and Birefringence Values of Xerogels Obtained from 1 in THF in the Presence of TBAF

xerogels	precursor concentration (mol L^{-1})	catalyst (mol %)	temperature (°C)	t_{gel} (min)	^{29}Si CP MAS NMR (%) T^0	T^1	T^2	T^3	L.C.[a] (%)	birefringence Δn ($\times 10^3$)
X1	1	2	20	1	0	0	44	56	85	1.7
X2	1	0.5	20	20	0	5	51	44	80	2.1
X3	1	0.2	20	90	0	6	49	45	80	2.6
X4	3	0.5	20	8	0	5	36	59	85	2.2
X5	3	0.2	20	45	0	5	42	53	83	2.7
X6	1	0.2	3	14[b]	10	23	42	25	61	3.2

[a] Level of condensation calculated according to the general equation L.C. = [0.5(T^1 area) + 1.0(T^2 area) + 1.5(T^3 area)]/1.5. [b] Days.

in 90% yield. Finally, a methanolysis of **3** in the presence of triethylamine gave the precursor **P** as a yellow oil in 83% yield.

Sol–Gel Processing of P. Gel formation from **P** has been examined under various reaction conditions. The hydrolysis–polycondensation reactions were performed in THF solutions in the presence of a nucleophilic catalyst (tetrabutylammonium fluoride, TBAF) (Scheme 4). Two different concentrations of precursor (1 and 3 M) and three ones of catalyst (0.2, 0.5, and 2 mol %) were employed. The influence of temperature was investigated in one case (Table 1). Translucent gels formed within various periods of time. The longer gel times were observed for the lower concentrations of catalyst (**X3** and **X2**) and at low temperature (**X6**). The gels were allowed to age for 6 days and were then powdered and washed with ethanol, acetone, and diethyl ether and dried in a vacuum (10^{-2} mmHg) at 120 °C for 2 h.

Spectroscopic Characterization and Textural Data for Xerogels. The solids were analyzed by ^{29}Si CP MAS NMR spectroscopy. When the hydrolysis–polycondensation was performed at 20 °C, the spectra displayed two main resonances at ca. −57 and ca. −65 ppm, assigned respectively to T^2 and T^3 substructures, and one very weak signal at ca. −48 ppm attributable to T^1 substructures. CP MAS is generally not quantitative; however, when compared with single-pulse experiments that allow a quantitative determination, no significant variation in relative peak intensity was observed in the case of such alkylene or arylene hybrid solids.[36,37] Moreover, since materials of the same precursor are compared, it can be assumed that relative peak intensity can be used to show a variation of the level of condensation between them. The level of condensation was estimated by deconvolution of spectra.[36,37] It was in the range 80–85% (Table 1). In contrast, when the reaction was performed at low temperature, the xerogel **X6** was poorly polycondensed (in the range of 60%) and T^0, T^1, T^2, and T^3 units were present. Nitrogen BET measurements[38,39] gave no significant specific surface areas (<10 m^2 g^{-1}) in all cases.

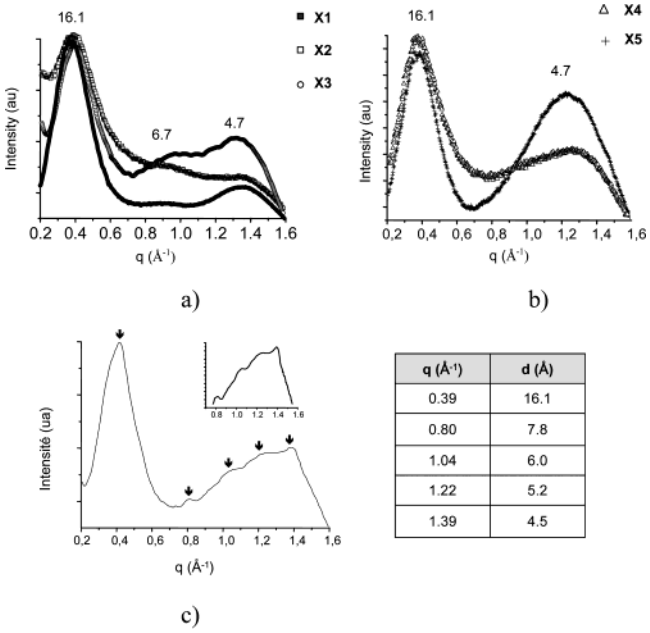

q (Å^{-1})	d (Å)
0.39	16.1
0.80	7.8
1.04	6.0
1.22	5.2
1.39	4.5

Figure 1. X-ray powder diffraction diagrams of the xerogels. (a) **X1**–**X3**; (b) **X4**–**X5**; (c) **X6**.

X-ray Powder Diffraction Analysis. The X-ray powder diffraction analysis of these materials was performed to obtain information on the organization at the nanometric scale. The diagrams are given in Figure 1. Like for all the other nanostructured hybrid materials reported until now,[30] the X-ray diffraction diagrams did not exhibit any sharp Bragg's signal. However, broad signals were observed and it is well-known that these broad signals correspond to the existence of a short-range order in the material. This point is very important since it means that a twisted and nonrigid precursor is able to induce a self-organization in the solid. As a first approximation assuming Bragg's law a priori, the distances associated with the q values were evaluated ($d = 2\pi/q$). A strong and broad signal was observed at 0.39 $Å^{-1}$ (16.1 Å). This signal could be attributed to a periodic distance due to the organic moiety; however, it

(36) Cerveau, G.; Corriu, R. J. P.; Lepeytre, C.; Mutin, P. H. *J. Mater. Chem.* **1998**, *8*, 2707.
(37) Oviatt, H. W., Jr.; Shea, K. J.; Small, J. H. *Chem. Mater.* **1993**, *5*, 943.
(38) Gregg, S. J.; Sing, S. W. *Adsorption, Surface Area and Porosity*; Academic Press: London, 1982.
(39) Brunauer, S.; Emmett, P. H.; Teller, E. J. *J. Am. Chem. Soc.* **1938**, *60*, 309.

Table 2

Organic part		Theoretical length[a] (Å)	Experimental Length (Å)
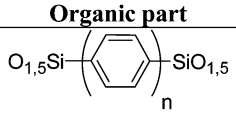			
n = 1	Si-Si	6.57	7.5
	O-O	7.65	
n = 2	Si-Si	10.83	12.5
	O-O	11.91	
n = 3	Si-Si	15.09	15.5
	O-O	16.18	
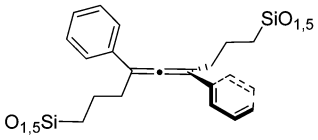			
	Si-Si	12.35	16.1
	O-O	13.82	

[a] Determined by computer simulation.

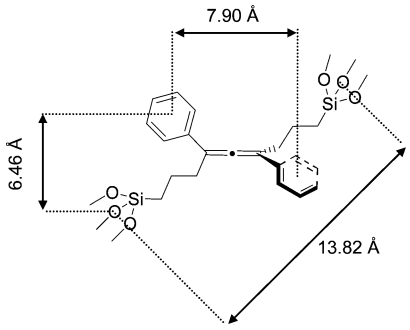

Figure 2.

was difficult to correlate this value with a distance characterizing the precursor as determined by computer simulation (Figure 2). Similarly, a broad signal centered at 4.7 Å was present in all cases. At present it is difficult to attribute this signal. However, it is possible to point out that the broad signals in the range of 4−5 Å are always observed in the case of precursors having a nonrigid linear geometry, planar or flexible, for instance.[40] It is interesting to compare the signal observed here with those obtained with linear rigid-rod precursors for which there is a clear correlation between the X-ray signal and the length of the spacer (Table 2).

The other observations are in agreement with the fact that all these materials are kinetically controlled as already demonstrated.[25,29] In the case of **X1**−**X3** an additional weak and broad signal was detected at a distance of ∼6.7 Å; it was not observed for **X4** and **X5,** which were prepared with a higher concentration of precursor. Interestingly, at low temperature (3° C-**X6**) the X-ray diagram exhibited additional weak signals, which might be indicative of a better organization (Figure 1). A study concerning the effect of temperature on the structure of this kind of material is in progress.

(40) Cerveau, G.; Corriu, R. J. P.; Framery, E.; Lerouge, F. *J. Mater. Chem.* **2004**, in press.

Birefringence Measurements. A small part of the starting mixtures was introduced separately into thin Teflon-coated cells.[41] Other coatings were previously tested but Teflon was chosen due to its chemical stability.[41] The initial solutions were completely dark when analyzed by polarized optical microscopy; this observation is characteristic of an isotropic medium. All the gels formed were transparent (the gel formation was evidenced by the absence of hydrodynamic movement), allowing a clear observation and measurements of the birefringence. The values for birefringence are given in Table 1. Pictures of the cells clearly showed the presence of bright pieces of solids separated by dark zones (Figure 3a, b, c). In the case of gels **X1**−**X3** prepared at 20 °C, the formation of cracks occurred a few hours after the formation of the gels in the cells. The intensity of birefringence was low and increased slowly to become stable after 1 week. No changes occurred after several months. The pictures of **X1** given in Figures 3a and 4 show clearly the presence of parallel wavy cracks. The picture of Figure 4 has been made at the smaller scale that can be recorded with the polarizing microscope. It is possible to notice the great regularity of propagation of the cracks on distances above 1.5 mm. Furthermore, a period of the waves could be estimated in the range 150−200 μm with an average value of 155 μm. This type of wave has never been reported previously. The orientation of the optical axis has been determined using a Berek compensator. It represents the average orientation of the organic moieties. The Figure 3a′ shows that this axis is oriented parallel to the edges of the cracks as previously observed.[41,42]

When the gels were prepared with a higher concentration of precursor (xerogels **X4** and **X5**), the situation

(41) Boury, B.; Corriu, R. J. P.; Le Strat, V.; Delord, P.; Nobili, M. *Angew. Chem., Int. Ed.* **1999**, *38*, 3172.

(42) Vergnes, A.; Nobili, M.; Delord, P.; Cipelletti, L.; Corriu, R. J. P.; Boury, B. *J. Sol-Gel Sci. Technol.* **2003**, *26*, 621.

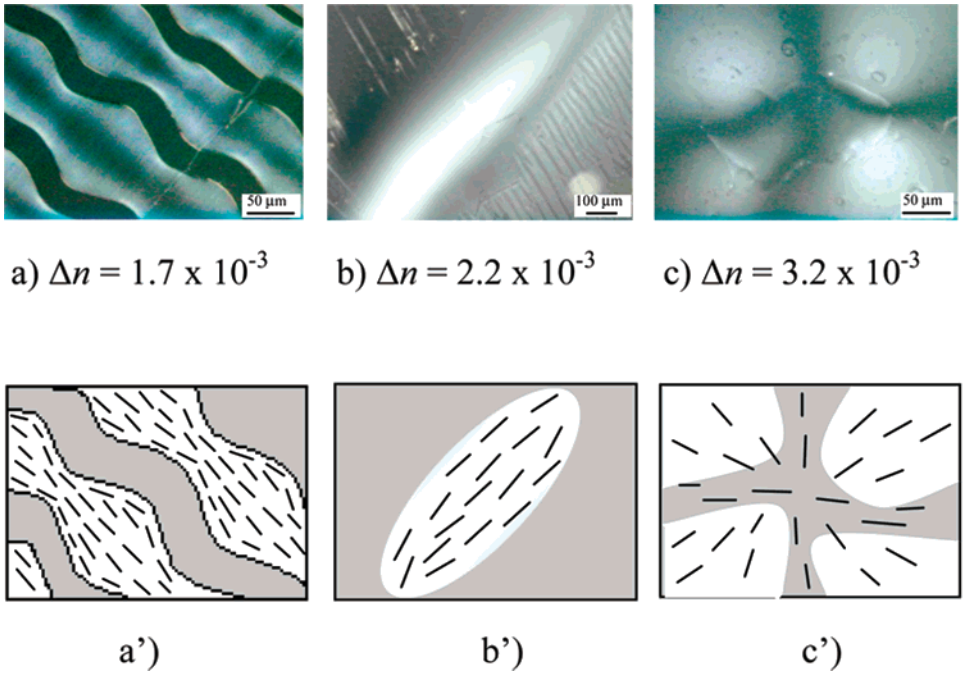

Figure 3. Xerogels observed by polarizing optical microscopy. (a) **X1**, (b) **X4**, and (c) **X6** and orientation of the optical axis, (a′) **X1**, (b′) **X4**, and (c′) **X6**.

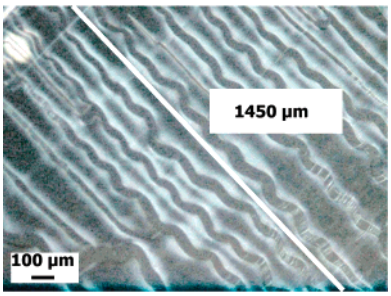

Figure 4. **X1** observed by polarizing optical microscopy at a different focus.

was different and the birefringence appeared without cracks after 5 days and its intensity was stabilized after 15 days. Figure 3b shows the crack-free xerogel with regions of lower and higher intensity. The average intensity lays in the same range as that of xerogels **X1**−**X3**. The orientation of the optical axis was in this case parallel to the zone of transition between the regions of different intensity as shown in Figure 3b. These observations and the results obtained with the mesogenic precursors[31] show that the stress/relaxation process cannot be proposed as the only controlling factor for birefringence formation.[26,27]

When the solid was prepared at 3 °C (**X6**), the birefringence appeared without cracks and was accompanied by the detachment of the gel from the walls of the cell, which corresponds to the densification of the solid due to polycondensation. Finally, the intensity was stable after 1 month. Interestingly, the longer the gel time, the higher the value for birefringence (**X6**). The optical axis was oriented radially around a central point (Figure 3c). This phenomenon of absence of cracks could originate from a stress due to the detachment of the gel during aging, which induced this particular orientation of the optical axis.

The temperature appeared to be an important parameter for organization since at 3 °C the solids were better organized at both the nanometric (X-ray) and micrometric scale (birefringence). Furthermore, the morphology of the cracks appeared to deeply depend on the concentrations of both the catalyst and the precursor.

Conclusion

The results presented here strengthen the fact that the auto-organization observed during the polycondensation of nanostructured organic−inorganic hybrid materials is induced by the weak interactions (van der Waals, London, or $\pi-\pi$ stacking) existing between the organic units during the polycondensation. In the case presented here, the "twisted" organic units present parameters of auto-organization totally different from that of the systems previously studied (linear, rigid, or semirigid). In the previous cases, the nanometric scale organization, evidenced by X-ray diffraction experiments, is related to the length of the organic spacer. The solids studied here present an unquestionable organization in view of the X-ray diagrams and the birefringence figures. However, the organization is different from the previous ones. This might probably be due to the fact that the interactions between the organic units with a twisted geometry induce a different arangement of the organic groups. It is interesting to note that the birefringence is unique. Liquid crystals with such a geometry have never been obtained.

Acknowledgment. The authors are very grateful to Prof. Pierre Delord and Dr. Philippe Dieudonné of the Department of Physics for fruitful discussions about the X-ray diffraction analysis.

CM049061C